Supporting material for "The influence of Ca^{2+} buffers on free [Ca^{2+}] fluctuations and the effective volume of Ca^{2+} microdomains"

Seth H. Weinberg and Gregory D. Smith

Department of Applied Science, The College of William & Mary,
Williamsburg, VA 23187, USA

SUPPORTING RESULTS

Validation of the linear noise approximation

To validate our analytical analysis, we performed Monte Carlo simulation of Ca^{2+} and buffer dynamics in a microdomain using Gillespie's stochastic simulation algorithm, an exact simulation algorithm that accounts for the small system size (1). We found close agreement between the coefficient of variation of the domain $[Ca^{2+}]$ fluctuations calculated from the linear noise approximation and the Monte Carlo simulations (Figure S1), in particular reproducing the bell-shaped dependence on total buffer concentration b_T^∞.

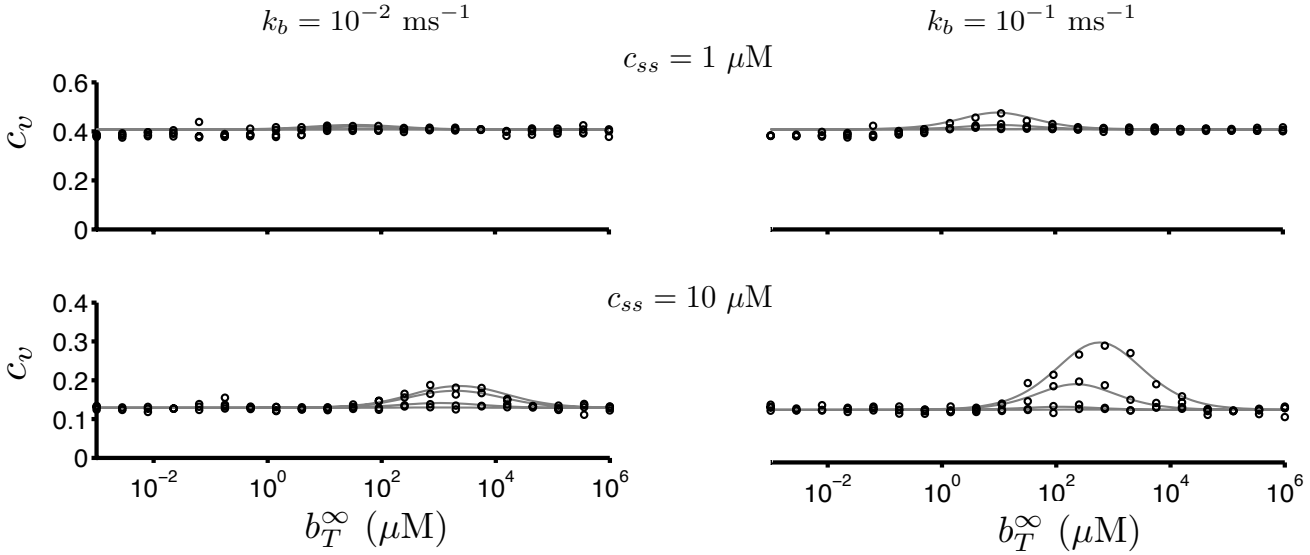

Figure S1: Comparison of the relative magnitude of domain $[Ca^{2+}]$ fluctuations, the coefficient of variation c_v, calculated using the linear noise approximation (solid gray lines), computed numerically using Eq. 32, and the exact value, determined from the ensemble average of 1000 Gillespie-type stochastic simulations (black circles). Parameters as in Figure 2.

$[Ca^{2+}]$ fluctuations in the presence of multiple buffers

The fluctuating RBA (Eq. 37) is readily generalizable to multiple buffers. For N rapid buffers with parameters b_T^n, κ_n, and k_b^n for $n \in \{1, \ldots, N\}$, the variance of the domain $[Ca^{2+}]$ fluctuations is given by

$$\sigma_c' = \frac{c_{ss}}{\Omega} \cdot (1 + \chi) \qquad \chi = \beta_{ss} \cdot \frac{\displaystyle\sum_{n=1}^{N} \frac{w_{ss}^n k_b^n}{c_\infty + \kappa_n}}{k_c + \displaystyle\sum_{n=1}^{N} w_{ss}^n k_b^n} \cdot (c_{ss} - c_\infty) \tag{S1}$$

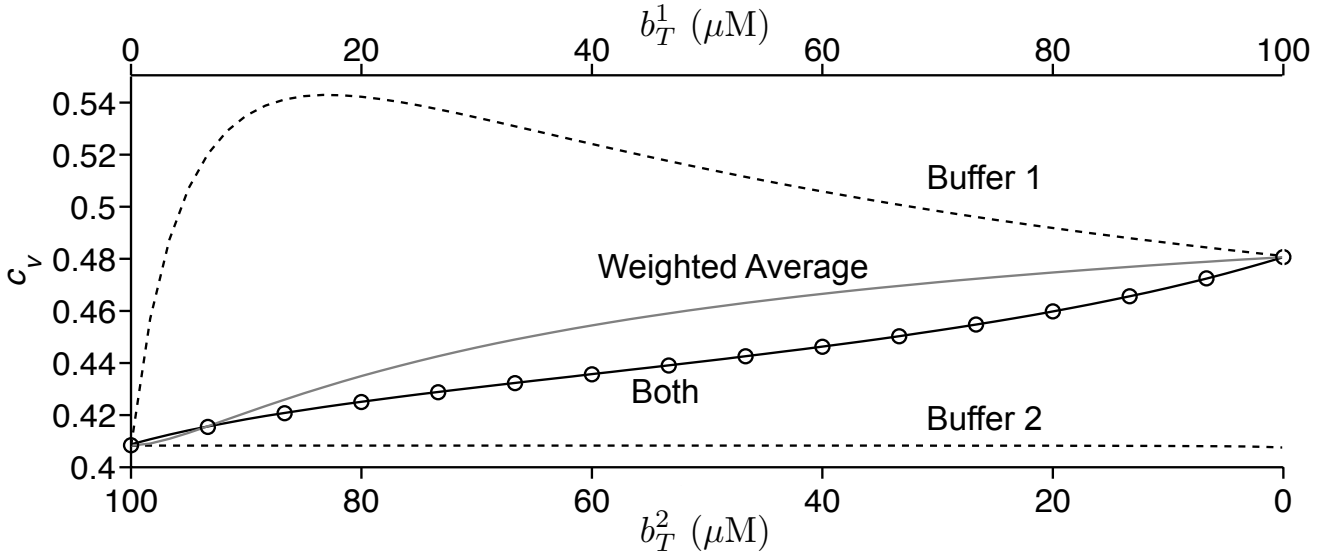

Figure S2: Combined influence of two rapid buffers on the coefficient of variation of domain $[Ca^{2+}]$ fluctuations (c_v) as the total concentration of buffer 1 (b_T^1) and buffer 2 (b_T^2) are varied with constant total amount of buffer ($b_T^1 + b_T^2 = 100$ μM). The fluctuating RBA (solid black line, Eq. S1) agrees with numerical solution of the full model (Eq. 30, open circles). The c_v in the presence of either buffer 1 or 2 in isolation (dashed lines) and a weighted average based on total buffer concentration (solid gray line) are also shown. Parameters: $c_{ss} = 1$ μM, $c_\infty = 0.1$ μM, $k_c = 0.2$ ms^{-1}, $\Omega = 10^{-17}$. Buffer 1: $k_+ = 10^2$ μM^{-1} ms^{-1}, $\kappa = 0.1$ μM, $k_b = 10^{-1}$ ms^{-1}. Buffer 2: $k_+ = 10^2$ μM^{-1} ms^{-1}, $\kappa = 1$ μM, $k_b = 10^{-3}$ ms^{-1}.

where β_{ss} and w_{ss}^n are

$$\beta_{ss} = \left(1 + \sum_{n=1}^{N} w_{ss}^n\right)^{-1} \quad \text{and} \quad w_{ss}^n = \frac{b_T^n \kappa_n}{(c_{ss} + \kappa_n)^2}, \tag{S2}$$

and for readability we have dropped the superscripted ∞ in the notation for total buffer concentration ($b_T^n \equiv b_T^{\infty,n}$).

Figure S2 shows the c_v for domain $[Ca^{2+}]$ fluctuations in the presence of two rapid buffers with different dissociation constants ($\kappa_2 > \kappa_1$) and exchange rates ($k_b^2 > k_b^1$). Moving left to right, the total concentration of buffer 1 (b_T^1) increases and the total concentration of buffer 2 (b_T^2) decreases, while the sum is held constant ($b_T^1 + b_T^2 = 100$ μM). The fluctuating RBA (Eq. S1, solid line) is in agreement with full calculations based on the appropriate generalization (Eq. 30, open circles), that is, the numerical solution of a Lyapunov equation composed of 5×5 known matrices H_{ss} and Γ_{ss}, and the symmetric 5×5 matrix Σ_{ss}, the steady-state covariance matrix for the fluctuating concentrations in the presence of two buffers, representing 10 unknown covariances. For comparison, Figure S2 shows the c_v obtained when buffer 1 or, alternatively, buffer 2 is included (dashed lines), as well as a weighted average of these values utilizing the total buffer concentrations ($b_T^i/(b_T^1 + b_T^2)$). As expected, this naive weighted average does not agree with the full calculation (circles), because the correct weighting is as implied by the fluctuating RBA (solid line, Eq. S1).

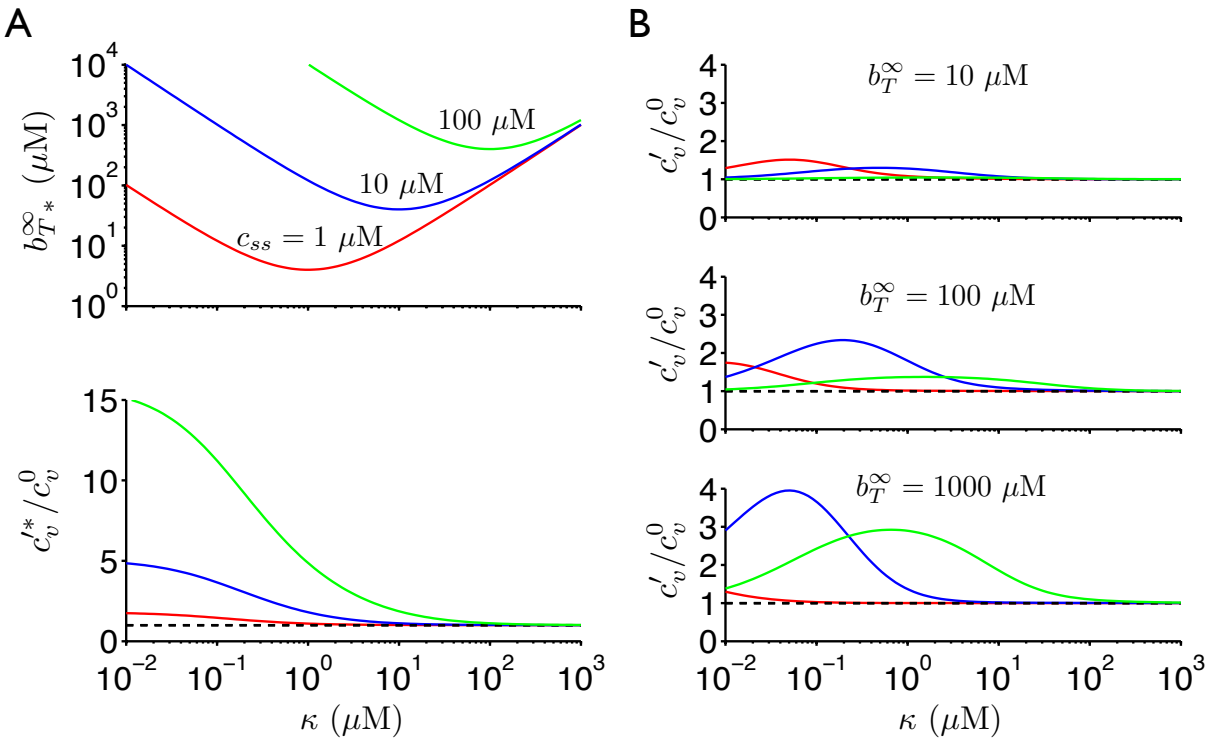

Figure S3: Dependence of $[Ca^{2+}]$ fluctuations on dissociation constant κ. (A, top) The total buffer concentration that maximizes $[Ca^{2+}]$ fluctuations (b^{∞}_{T*}) for a fixed steady-state $[Ca^{2+}]$, c_{ss} (Eq. 42). (A, bottom) The enhancement of $[Ca^{2+}]$ fluctuations, $c_v'^*/c_v^0$, that occurs with optimal total buffer concentration (b^{∞}_{T*}) as a function of the buffer dissociation constant κ (Eq. 43). (B) The enhancement of $[Ca^{2+}]$ fluctuations, c_v'/c_v^0, for different values of c_{ss} and b_T^{∞} (Eq. 40) plotted as functions of κ. Parameters: $c_{\infty} = 0.1$ μM, $k_c = k_b = 0.2$ ms^{-1}.

Influence of the buffer dissociation constant κ on $[Ca^{2+}]$ fluctuations

The buffer dissociation constant κ influences buffer-mediated increase in $[Ca^{2+}]$ fluctuations in a complex manner. For example, the variance of free $[Ca^{2+}]$ fluctuations (σ_c', Eqs. 37 and 38) depends on the relative (as opposed to absolute) concentrations of domain (c_{ss}/κ) and bulk (c_{∞}/κ) Ca^{2+} and total buffer (b_T^{∞}/κ) via the dimensionless quantities β_{ss} and w_{ss}, because the later can expressed as $w_{ss} = (b_T^{\infty}/\kappa)/(1+c_{ss}/\kappa)^2$ and, similarly, the second factor of χ can be written as $(c_{ss}/\kappa - c_{\infty}/\kappa)/(1 + c_{\infty}/\kappa)$. However, an increase or decrease in κ does not simply shift the bell-shaped curves describing c_v vs. b_T^{∞} (as in Figure 2) to the left or right.

For a given steady-state $[Ca^{2+}]$, c_{ss}, the total buffer concentration with maximal effect (b^{∞}_{T*}, Eq. 42) is a u-shaped function of the buffer dissociation constant κ (Figure S3A, top). The value of κ that *minimizes this optimal total buffer concentration* is found as the κ that zeros $\partial b^{\infty}_{T*}/\partial\kappa$ and is given by $\kappa = c_{ss}$. This suggests that as c_{ss} increases, weaker affinity (i.e., larger κ) buffers are more effective at enhancing domain $[Ca^{2+}]$ fluctuations. However, for a given value of c_{ss}, a buffer with dissociation constant $\kappa = c_{ss}$ does not necessarily enhance domain $[Ca^{2+}]$ fluctuations to the greatest extent possible, as the fluctuation enhancement is a decreasing function of κ (given by $c_v'^*/c_v^0$, Eq. 43, Figure S3A, bottom).

In order to determine an optimal dissociation constant κ_* that maximizes domain $[Ca^{2+}]$ fluctuations, it is instructive to plot the fluctuation enhancement, c_v'/c_v^0 (Eq. 40) for a given fixed c_{ss} and total buffer concentration b_T^∞ (Figure S3B). These curves are bell-shaped functions of κ: for both small κ (high affinity buffer) and large κ (low affinity buffer), steady-state buffering capacity $w_{ss} \to 0$ (Eq. 38) and, consequently, $c_v'/c_v^0 \approx 1$. For a given c_{ss} and b_T^∞, the optimal dissociation constant κ_* (corresponding to the peak of the bell-shaped curve) is found as the κ that zeros $\partial\chi/\partial\kappa$. This optimal dissociation constant is the positive solution of the quartic equation,

$$\kappa_*^4 + a\kappa_*^3 + b\kappa_*^2 + c\kappa_* + d = 0, \tag{S3}$$

where

$$\begin{aligned} a &= \tfrac{1}{2}\left(c_\infty + 4c_{ss}\right) \\ b &= \tfrac{1}{2}\left[c_{ss}\left(b_T^\infty + 2c_{ss} + c_\infty\right) + b_T^\infty\left(c_{ss} - c_\infty\right)\right] \\ c &= \tfrac{1}{2}c_{ss}c_\infty(b_T^\infty - c_{ss}) \\ d &= -\tfrac{1}{2}c_\infty c_{ss}^3. \end{aligned}$$

Figure S3 shows that for fixed b_T^∞, κ_* is an increasing function of c_{ss}, that is, when c_{ss} is large, fluctuations are enhanced to the largest extent by low affinity buffers. For a given c_{ss}, κ_* is a decreasing function of b_T^∞. Figure S3 shows that domain $[Ca^{2+}]$ fluctuations may be enhanced several-fold for physiological values of b_T^∞ and κ, especially for larger values of $c_{ss} = 10$ and 100 μM.

Time scale of domain $[Ca^{2+}]$ fluctuations

Figure S4 characterizes the time scale of $[Ca^{2+}]$ fluctuations by plotting the domain $[Ca^{2+}]$ auto-correlation function, denoted by $\phi_{c,c}(\tau)$ in Eq. 45, for a range of model parameters. In brief, our calculations suggest that in the presence of rapid, high concentration buffer, the time scale of domain $[Ca^{2+}]$ fluctuations may range over several orders of magnitude (0.1 μs to 10 ms), depending on the steady-state domain $[Ca^{2+}]$.

For low domain $[Ca^{2+}]$ ($c_{ss} = 0.1$ μM) and total buffer (b_T^∞) concentrations (top row), a semi-logarithmic plot of the autocorrelation function $\phi_{c,c}$ is a decreasing sigmoid with 50% decay $\sim$1 ms, as in the absence of buffer (dashed black lines). As b_T^∞ increases, the characteristic time scale of $[Ca^{2+}]$ fluctuations decreases ($\phi_{c,c}$ shifts to the left). For example, for a slow buffer at total concentration of $b_T^\infty = 10^4$ μM (blue), the time scale is $\sim$0.1 ms (Figure S4A, top panel). For a fast buffer, the influence of b_T^∞ is more pronounced, for example, when $b_T^\infty = 10^4$ μM (blue), the time scale is $\sim 10^{-4}$ ms (Figure S4B, top panel).

For large steady-state domain $[Ca^{2+}]$, the autocorrelation function $\phi_{c,c}$ is a decreasing (double) sigmoid with two "knees," indicating that $[Ca^{2+}]$ fluctuations are characterized by two distinct time scales. For example, for a fast buffer, $c_{ss} = 10$ μM, and $b_T^\infty = 10^4$ μM (blue), the two time scales are $\sim 10^{-3}$ and 10 ms (Figure S4B, third panel) that may correspond to the buffer kinetics and exchange rates, respectively (see Figure S5).

As c_{ss} increases further, the fast time scale (small τ) becomes less prominent and the slow time scale (large τ) dominates. These effects are more pronounced when buffers are rapid (right column). Increasing the buffer exchange rate k_b has minimal influence on the shape of $\phi_{c,c}$, but does increase the values of b_T^∞ that lead to dominance of the show time scale (not shown).

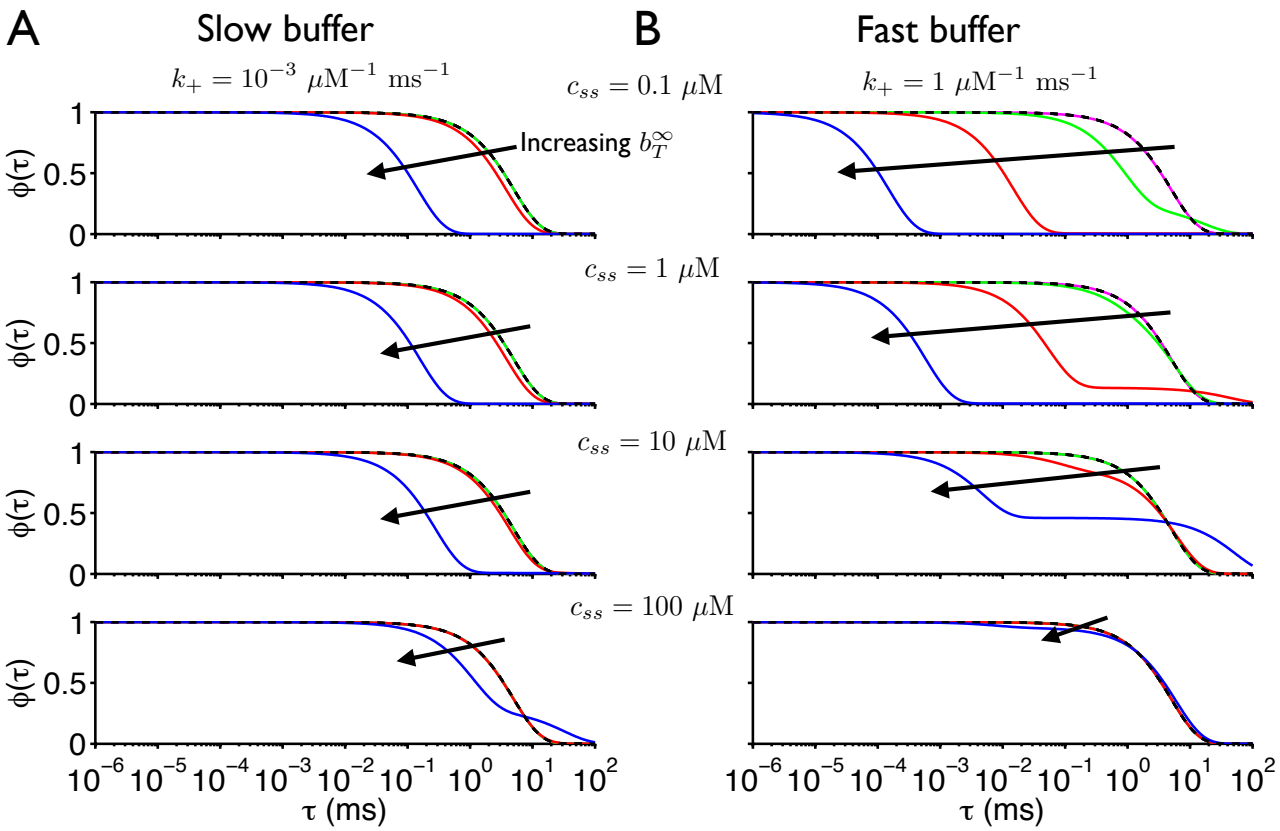

Figure S4: Dependence of the auto-correlation function $\phi_{c,c}(\tau)$ on steady-state domain $[Ca^{2+}]$ (c_{ss}) and total buffer concentration (b_T^∞) (Eq. 45). Parameters: $c_\infty = 0.1$ μM, $\kappa = 0.2$ μM, $\Omega = 10^{-17}$ L, $k_c = 0.2$ ms^{-1}, $k_b = 10^{-2}$ ms^{-1}, $b_T^\infty = 0$ (no buffer, dashed black), 10^{-2} (magenta), 1 (green), 10^2 (red) and 10^4 (blue) μM.

The physical processes that correspond with the observed knees in the autocorrelation functions plotted in Figure S4 can be identified to some extent but not isolated. The relaxation time of fluctuations is governed by the eigenvalues of the steady-state Jacobian matrix H_{ss}. In fact, the relevant rates are (up to a sign change) given by the six pairwise sums of the eigenvalues of the Jacobian matrix H_{ss} (three eigenvalues with negative real parts). To see this, note that that Eq. 27,

$$\dot{\Sigma} = H_{ss}\Sigma + \Sigma H_{ss}^T + \Gamma_{ss},$$

can be written as

$$\frac{d}{dt}\text{vec}(\Sigma) = (H_{ss} \oplus H_{ss})\text{vec}(\Sigma) + \text{vec}(\Gamma_{ss}), \tag{S4}$$

where $\oplus$ is a Kronecker sum and the vec operation creates a column vector from a matrix by stacking its column vectors. It is well-known (2) that if $A \in \mathbb{R}^{n\times n}$ has eigenvalues λ_i for $i = 1, \ldots, n$ and $B \in \mathbb{R}^{m\times m}$ has eigenvalues $\mu_j = 1, \ldots, m$, then $A \oplus B$ has mn eigenvalues,

$$\lambda_1 + \mu_1, \ldots, \lambda_1 + \mu_m, \lambda_2 + \mu_1, \ldots, \lambda_2 + \mu_m, \ldots, \lambda_n + \mu_m.$$

Denoting the three eigenvalues of H_{ss} as λ_1, λ_2 and λ_3, it follows that $H_{ss} \oplus H_{ss}$ has eigenvalues

$$2\lambda_1,\ \lambda_1 + \lambda_2,\ \lambda_1 + \lambda_3,\ 2\lambda_2,\ \lambda_2 + \lambda_3,\ 2\lambda_3. \tag{S5}$$

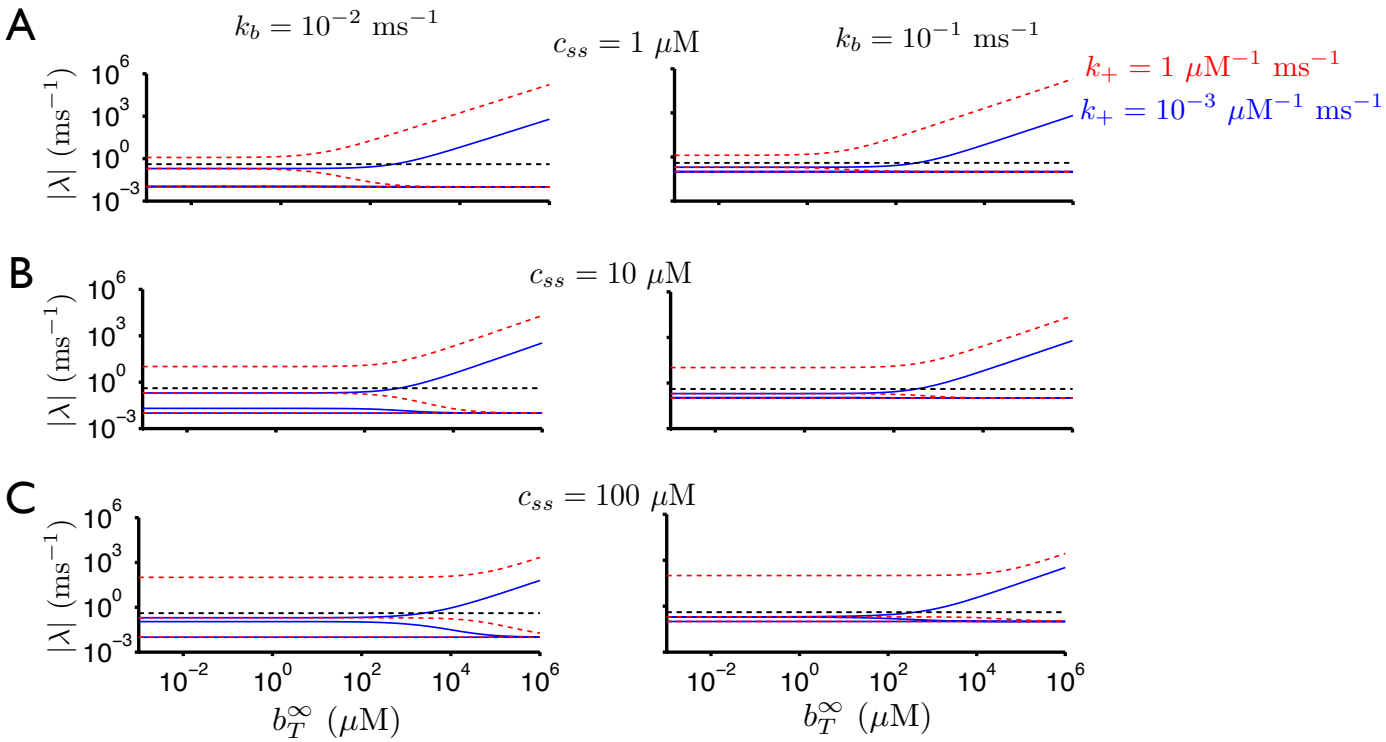

Figure S5: [Ca^{2+}] fluctuation relaxation rates ($|\lambda_i|$, $i \in \{1, 2, 3\}$) plotted as a function of buffer parameters (cf. Eq. S5 and nearby text). Horizontal dotted black line indicates rate in the absence of buffer ($2k_c$, Eq. 15). Parameters: $c_{ss} = 1$ (A), 10 (B), and 100 (C) μM, $c_\infty = 0.1$ μM, $\kappa = 0.2$ μM, $\Omega = 10^{-17}$ L, $k_c = 0.2$ ms^{-1}, $k_+ = 10^{-3}$ (solid blue) and 1 (dashed red) μM^{-1} ms^{-1}.

Figure S5 shows a numerical calculation of the relaxation rates derived from the eigenvalues of H_{ss} ($|\lambda_i|$, $i \in \{1, 2, 3\}$) and the dependence of these rates on Ca^{2+} buffer parameters. The rates range over several orders of magnitude (10^{-3} to 10^4 ms^{-1}). As total buffer concentration b_T^∞ increases, the fastest rate increases, the slowest rate remains constant, and the intermediate rate decreases (asymptotically approaching the slow rate). Increasing the rate of exchange of buffer between domain and bulk (k_b) increases the slow and intermediate rates, but does not change the fast rate (compare left and right panels). Increasing the buffer kinetics (k_+, k_-) increases the fast rate, but does not influence the slow and intermediate rate (compare solid blue and dashed red lines). The fastest rate is an increasing function of the steady-state domain [Ca^{2+}] (c_{ss}) (cf. A, B and C).

[Ca^{2+}] fluctuations during a time-varying Ca^{2+} influx

In the main text, we demonstrate that in the presence of a constant Ca^{2+} influx rate, buffers enhance the size of domain [Ca^{2+}] fluctuations around the non-equilibrium steady-state. Figure S6 illustrates an example of a time-varying Ca^{2+} influx rate, during which buffers do not suppress and may enhance domain [Ca^{2+}] fluctuations. In Figure S6A, Ca^{2+} influx rate is characteristic of triggered SR Ca^{2+} release, i.e., a Ca^{2+} spark (top panel, inset). Numerical simulations demonstrate that buffers increase intrinsic domain [Ca^{2+}] fluctuations during

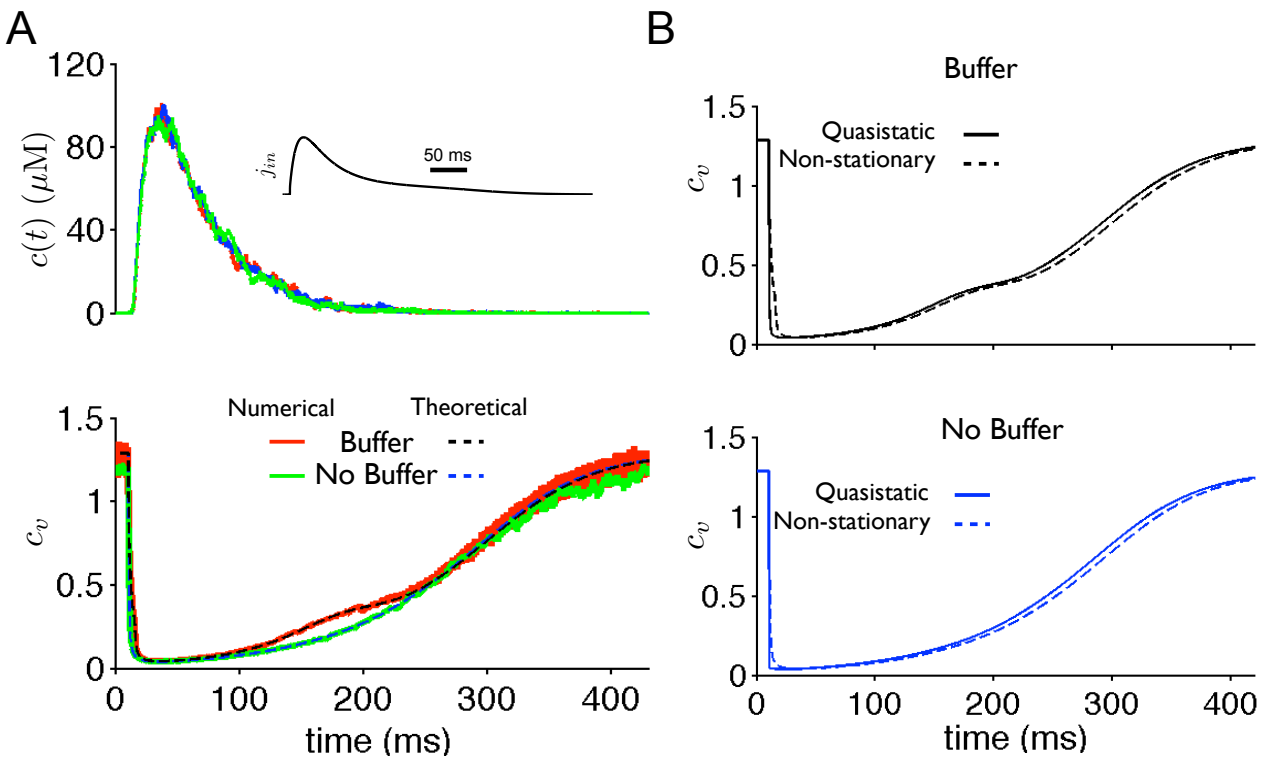

Figure S6: $[Ca^{2+}]$ fluctuations during a time-varying Ca^{2+} influx. (A, top) Monte Carlo simulations of domain $[Ca^{2+}]$, $c(t)$, in the presence of buffer and a time-varying Ca^{2+} influx, $j_{in}(t)$, generated by numerical integration of Eq. 21 using the Euler-Maruyama method. The time-varying $j_{in}(t)$ is characteristic of triggered SR Ca^{2+} release and given by an α-function, $j_{in}(t) \propto (\exp(-t/\tau_2) - \exp(-t/\tau_1))$ (see inset). (A, bottom) The ensemble domain $[Ca^{2+}]$ coefficient of variation, c_v, calculated from 1000 Monte Carlo simulations, in the presence (solid red) and absence (solid green) of buffer, is plotted throughout the time-varying Ca^{2+} influx. Theoretical calculation of c_v for non-stationary domain concentrations, determined from integration of Eq. 27 in the presence (dashed black) and absence (dashed blue) agree closely with the numerical simulations. (B) Theoretical calculation of c_v, for non-stationary (solid) and quasistatic (dashed) domain concentrations in the presence (top) and absence (bottom) of buffer. See text for details of the calculations. Note that the dashed black and dashed blue traces in (A) and (B) are the same. Parameters: $b_T^{\infty} = 50$ μM, $c_{\infty} = 0.1$ μM, $\kappa = 0.2$ μM, $k_c = 0.2$ ms^{-1}, $k_b = 0.1$ ms^{-1}, $k_+ = 1$ μM^{-1} ms^{-1}, $\Omega = 10^{-17}$ L, $\tau_1 = 10$ ms, $\tau_2 = 40$ ms.

systole, and buffers do not suppress $[Ca^{2+}]$ fluctuations during diastole (A, bottom, solid red and green).

A calculation of the domain $[Ca^{2+}]$ fluctuations during a time-varying Ca^{2+} influx rate $j_{in}(t)$ can be obtained by numerical integration of Eq. 27 (3),

$$\dot{\Sigma} = H\Sigma + \Sigma H^T + \Gamma,$$

where the Jacobian matrix H and two-time covariance matrix Γ are evaluated at the time-varying expected value of the domain Ca^{2+} and buffer concentrations, i.e., $c(t)$, $b(t)$, and

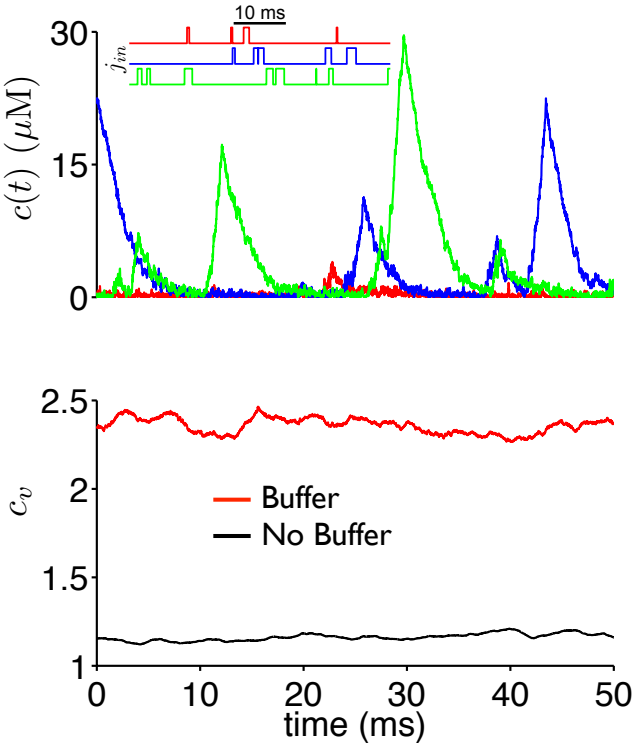

Figure S7: $[Ca^{2+}]$ fluctuations during a stochastically-gated Ca^{2+} influx. (top) Monte Carlo simulations of domain $[Ca^{2+}]$, $c(t)$, in the presence of buffer and a time-varying Ca^{2+} influx, $j_{in}(t)$, generated by numerical integration of Eq. 21 using the Euler-Maruyama method. The time-varying $j_{in}(t)$ is stochastically gated with a mean open time of 1 ms and mean closed time of 9 ms (see inset). (bottom) The ensemble domain $[Ca^{2+}]$ coefficient of variation, c_v, calculated from 1000 Monte Carlo simulations, in the presence (red) and absence (black) of buffer, is plotted throughout the time-varying Ca^{2+} influx. Parameters: $b_T^{\infty} = 50$ μM, $c_{\infty} = 0.1$ μM, $\kappa = 0.2$ μM, $k_c = 0.2$ ms^{-1}, $k_b = 0.1$ ms^{-1}, $k_+ = 1$ μM^{-1} ms^{-1}, $\Omega = 10^{-17}$ L.

$cb(t)$, found by numerical integration of Eq. 19. Non-stationary calculations agree closely with numerical simulations in the presence (Figure S6A, bottom, dashed black) and absence (dashed blue) of buffer. Alternatively, we may assume that the domain concentrations are in quasistatic equilibrium with the time-varying influx rate, i.e., $c_{ss}(t) = c_{ss}(j_{in}(t))$ and similarly for $b_{ss}(t)$ and $cb_{ss}(t)$ as determined by Eq. 20, and estimate $\Sigma(t)$ using the the fluctuation-dissipation theorem (Eq. 30, the steady-state of Eq. 27) and the quasistatic values of $\Gamma_{ss}(t)$ and $H_{ss}(t)$. Figure S6B shows that this approximation deviates only slightly from the aforementioned non-stationary calculation, and thus both theoretical methods yield results in close agreement with stochastic simulation.

We also show Monte Carlo simulations of $[Ca^{2+}]$ during a stochastically gated influx (Figure S7). The stochastically gated influx has mean open time of 1 ms and mean closed time of 9 ms. Throughout the time course, $[Ca^{2+}]$ fluctuations in the presence of buffer (red) are larger compared with in the absence of buffer (black).

SUPPORTING APPENDICES

Appendix A: The chemical Langevin equation and linear noise approximation

Consider a well-stirred compartment with $\mathcal{I}$ chemical species undergoing elementary reactions indexed by q. The q-th elementary reaction can be characterized by (a) the forward and backward reaction rates per unit volume, $\nu_q^+(\boldsymbol{\rho})$ and $\nu_q^-(\boldsymbol{\rho})$, that may depend on species concentrations $\boldsymbol{\rho}(t) = (\rho_1, \rho_2, \cdots, \rho_{\mathcal{I}})^T$, and (b) the change in the number of molecules when the q-th reaction occurs, denoted by the column vector $\boldsymbol{\omega}_q = (\omega_{q\,1}, \omega_{q\,2}, \cdots, \omega_{q\,\mathcal{I}})^T$, a difference of stoichiometric coefficients (products minus reactants).

If $\boldsymbol{N}(t) = (N_1, N_2, \cdots, N_{\mathcal{I}})^T$ (a random vector) is the copy number of each species at time t, the probability distribution $W(\boldsymbol{n}, t) = \Pr\{\boldsymbol{N}(t) = \boldsymbol{n}\}$ solves the *chemical master equation*:

$$\begin{aligned}\frac{d}{dt}W(\boldsymbol{n},t) = &\sum_q V_q^+(\boldsymbol{n}-\boldsymbol{\omega}_q)W(\boldsymbol{n}-\boldsymbol{\omega}_q,t) + V_q^-(\boldsymbol{n}+\boldsymbol{\omega}_q)W(\boldsymbol{n}+\boldsymbol{\omega}_q,t)\\ &- \sum_q [V_q^+(\boldsymbol{n}) + V_q^-(\boldsymbol{n})]W(\boldsymbol{n},t),\end{aligned} \tag{S6}$$

where $V_q^{\pm}(\boldsymbol{n}) = \Omega\,\nu_q^{\pm}(\boldsymbol{n}/\Omega)$ are the forward and backward reaction rates for the q-th elementary reaction. The chemical master equation is a system of ODEs, one for each possible state. Often the high dimensionality of the chemical master equation makes its use prohibitive. Several approaches have been utilized to show that for sufficiently large system size and reaction rates, the stochastic dynamics of the species concentrations ρ_i are well-approximated by solutions of the *chemical Langevin equation* (4-6),

$$\dot{\rho_i} = \sum_q \omega_{q\,i}(\nu_q^+ - \nu_q^-) + \xi_i(t) \tag{S7}$$

where the column vector of fluctuating forces, $\boldsymbol{\xi} = (\xi_1, \xi_2, \ldots, \xi_{\mathcal{I}})^T$, has mean zero

$$\langle \xi_i(t) \rangle = 0, \qquad i = 1, 2, \ldots, \mathcal{I} \tag{S8}$$

and two-time covariance

$$\langle \boldsymbol{\xi}(t)\,\boldsymbol{\xi}^T(t') \rangle = \Gamma(\boldsymbol{\rho})\delta(t-t'). \tag{S9}$$

where the general form of the two-time covariance matrix, $\Gamma = (\gamma_{ij})$, is given by (3)

$$\gamma_{ij} = \Omega^{-1} \sum_q \omega_{q\,i}\,(\nu_q^+ + \nu_q^-)\,\omega_{q\,j}, \tag{S10}$$

that is, the covariance γ_{ij} is the sum of forward and backward reaction rates, multiplied by the change in copy number of species i and j, summed over each reaction q and scaled by the inverse of domain volume Ω.

Assuming a stable steady state $\boldsymbol{\rho}^{ss} = \boldsymbol{n}^{ss}/\Omega$, the linear noise approximation to Eq. S7 is

$$\dot{\delta\boldsymbol{\rho}} = H^{ss}\delta\boldsymbol{\rho} + \xi_i^{ss}(t) \tag{S11}$$

where the fluctuation $\delta\boldsymbol{\rho} = \boldsymbol{\rho}(t) - \boldsymbol{\rho}^{ss}$, the matrix $H^{ss} = (h_{ij}^{ss})$ is the Jacobian of reaction terms in the chemical Langevin equation (Eq. S7) evaluated at steady state, that is,

$$h_{ij}^{ss} = \left. \frac{\partial \sum_q \omega_{q\,i} \, \left[\nu_q^+(\boldsymbol{\rho}) - \nu_q^-(\boldsymbol{\rho})\right]}{\partial \rho_j} \right|_{\boldsymbol{\rho}=\boldsymbol{\rho}^{ss}} \tag{S12}$$

and $\xi_i^{ss}(t)$ has the same form as $\xi_i(t)$ in Eq. S7 with Γ evaluated at $\boldsymbol{\rho}^{ss}$. The approximations relating the chemical master equation, chemical Langevin equation, and linear noise approximation are subtle (3-7). The validity of these approximations depends on multiple factors, including reaction rates (propensities) and the number of molecules $n = \Omega c$, where c is a characteristic concentration for the species being simulated. Our use of the linear noise approximation was validated through comparison of the analytical and symbolic results (Eq. S11) to Gillespie-type stochastic simulation (Figure S1) that is an exact sampling of the steady-state probability distribution solving the chemical master equation (Eq. S6).

For the analysis of the fluctuations produced by Eq. S11, we consider an ensemble of identically prepared systems with $\boldsymbol{\rho}(0) = \boldsymbol{\rho}^{ss}$ or, equivalently, $\delta\boldsymbol{\rho}(0) = 0$, and numerically or analytically calculate the $\mathcal{I} \times \mathcal{I}$ symmetric covariance matrix

$$\Sigma(t) = \langle \delta\boldsymbol{\rho}(t) \, \delta\boldsymbol{\rho}^T(t) \rangle$$

that solves Eq. 27,

$$\dot{\Sigma} = H_{ss}\Sigma + \Sigma H_{ss}^T + \Gamma_{ss},$$

which follows from Eq. S11 and the definition of $\Sigma(t)$. We are primarily interested in the steady-state covariance matrix Σ_{ss} that solves the following Lyapunov equation, which relates Γ_{ss} and Σ_{ss} and is called the *fluctuation-dissipation theorem*,

$$H_{ss}\Sigma_{ss} + \Sigma_{ss}H_{ss}^T = -\Gamma_{ss}.$$

Appendix B: Derivation of the rapid buffer approximation

In this Appendix we derive a general analytical expression for the variance of the free $[Ca^{2+}]$ fluctuations in the presence of rapid Ca^{2+} buffer (Eq. 37) using Eqs. 34 and 36 as our starting point,

$$\dot{\delta c} = -\left[k_+(c_{ss} + b_{ss}) + k_- + k_c\right] \delta c + \left(k_+ c_{ss} + k_-\right) \delta c_T - k_+ c_{ss} \, \delta b_T + \xi_c^{ss}(t) \tag{S13a}$$

$$\dot{\delta c_T} = -\beta_{ss} \left(k_c + w_{ss} k_b\right) \delta c_T + \beta_{ss} \left(k_c - k_b\right) \nu_{ss} \, \delta b_T + \xi_{c_T}^{ss} \tag{S13b}$$

$$\dot{\delta b_T} = -k_b \delta b_T + \xi_{b_T}^{ss}, \tag{S13c}$$

where δc is the fast variable, δc_T and δb_T are slow variables, and we have written $\xi_{c_T}(t) = \xi_c(t) + \xi_{cb}(t)$ and $\xi_{b_T}(t) = \xi_b(t) + \xi_{cb}(t)$. Eq. S13b is derived using a quasistatic approximation for the average value of the $[Ca^{2+}]$ fluctuation (Eq. 35),

$$\langle \delta c \rangle_* \approx \beta_{ss} \left[\delta c_T - \nu_{ss} \, \delta b_T\right], \tag{S14}$$

where $\nu_{ss} = c_{ss}/(c_{ss} + \kappa)$ and $\langle \cdot \rangle_*$ indicates a time average (as opposed to an ensemble average). As a consequence, the reaction terms of Eq. S13b that involved the fast fluctuation

δc have been replaced by a time average that is a function of the slow fluctuations δc_T and δb_T, that is, the slow SDEs (Eqs. S13b and S13c) are now expressed in terms of the slow fluctuations.

The quasistatic approximation for δc (Eq. S14) is obtained from Eq. S13a by dividing both sides by $k_+\zeta_{ss}$ to yield

$$\frac{1}{k_+\zeta_{ss}}\dot{\delta c} = -\delta c + \beta_{ss}\left(\delta c_T - \nu_{ss}\,\delta b_T\right) + \frac{\xi_c^{ss}(t)}{k_+\zeta_{ss}},$$

where $\zeta_{ss} = c_{ss} + b_{ss} + \kappa + k_c/k_+$, $\kappa = k_-/k_+$, and we have used $(c_{ss}+\kappa)/\zeta_{ss} = \beta_{ss}$. In the rapid buffer limit ($k_+, k_- \to \infty$ with κ fixed) this expression becomes

$$0 = -\delta c + \beta_{ss}\delta c_T - \beta_{ss}\nu_{ss}\,\delta b_T,$$

where $\zeta_{ss} \to c_{ss} + b_{ss} + \kappa$ and $b_{ss} \to b_T\kappa/(c_{ss}+\kappa)$ (Eq. 20). Because this is an outer solution for a fluctuating quantity, for this zeroth order approximation we write

$$\langle \delta c\rangle_* \approx \beta_{ss}\left(\delta c_T - \nu_{ss}\,\delta b_T\right),$$

where $\langle\delta c\rangle_*$ is a time average, that is, an average of δc over an intermediate time scale, long compared to the fluctuations in $\xi_c(t)$, but short compared to the relaxation time for the slow variables δc_T and δb_T.

The steady-state covariances of the slow subsystem (Eqs. S13b and S13c) are found by solving the 2×2 Lyapunov equation (Eq. 30),

$$H_{ss}^{slow}\Sigma_{ss}^{slow} + \Sigma_{ss}^{slow}(H_{ss}^{slow})^T = -\Gamma_{ss}^{slow}, \tag{S15}$$

where the unknown symmetric matrix is

$$\Sigma_{ss}^{slow} \;=\; \begin{pmatrix} \langle \delta c_T^2\rangle & \langle \delta c_T\,\delta b_T\rangle \\ \star & \langle \delta b_T^2\rangle \end{pmatrix}$$

and the $\star$ indicates that $\langle \delta b_T\,\delta c_T\rangle = \langle \delta c_T\,\delta b_T\rangle$. Eq. S15 is expanded to yield three equations for three unknowns,

$$\begin{aligned}
2h_{c_Tc_T}^{slow}\langle\delta c_T^2\rangle + 2h_{c_Tb_T}^{slow}\langle\delta c_T\,\delta b_T\rangle &= -\gamma_{c_T\,c_T}^{ss} && \text{(S16a)}\\
(h_{c_Tc_T}^{slow} + h_{b_Tb_T}^{slow})\langle\delta c_T\,\delta b_T\rangle + h_{c_Tb_T}^{slow}\langle\delta b_T^2\rangle &= -\gamma_{c_T\,b_T}^{ss} && \text{(S16b)}\\
2h_{b_Tc_T}^{slow}\langle\delta c_T\,\delta b_T\rangle + 2h_{b_Tb_T}^{slow}\langle\delta b_T^2\rangle &= -\gamma_{b_T\,b_T}^{ss} && \text{(S16c)}
\end{aligned}$$

where the elements of the relaxation matrix H_{ss}^{slow} are (cf. Eq. 36),

$$\begin{aligned}
h_{c_Tc_T}^{slow} &= -\alpha_{ss} = -\beta_{ss}(k_c + k_b w_{ss}), && \text{(S17a)}\\
h_{c_Tb_T}^{slow} &= = (k_c - k_b)\,\beta_{ss}\,\nu_{ss} = (k_c - k_b)\,c_{ss}/\zeta_{ss}, && \text{(S17b)}
\end{aligned}$$

$h_{b_Tc_T}^{slow} = 0$ and $h_{b_Tb_T}^{slow} = -k_b$.

The 2×2 covariance matrix Γ_{ss}^{slow} for $\xi_{c_T}^{ss}$ and $\xi_{b_T}^{ss}$ is calculated using Eq. 23 and the relationships

$$\begin{aligned}
\langle \xi_{c_T}^2\rangle &= \langle\xi_c^2\rangle + 2\langle\xi_c\,\xi_{cb}\rangle + \langle\xi_{cb}^2\rangle && \text{(S18a)}\\
\langle \xi_{c_T}\,\xi_{b_T}\rangle &= \langle\xi_c\,\xi_b\rangle + \langle\xi_c\,\xi_{cb}\rangle + \langle\xi_{cb}\,\xi_b\rangle + \langle\xi_{cb}\,\xi_{cb}\rangle && \text{(S18b)}\\
\langle \xi_{b_T}^2\rangle &= \langle\xi_b^2\rangle + 2\langle\xi_b\,\xi_{cb}\rangle + \langle\xi_{cb}^2\rangle, && \text{(S18c)}
\end{aligned}$$

where we have dropped the superscripted ss for clarity. In this way we identify $\gamma^{ss}_{c_T\,c_T} = \gamma^{ss}_{c} + \gamma^{ss}_{cb}$, $\gamma^{ss}_{c_T\,b_T} = \gamma^{ss}_{cb}$ and $\gamma^{ss}_{b_T\,b_T} = \gamma^{ss}_{b} + \gamma^{ss}_{cb}$. Importantly, these expressions are independent of the rate constants k_+ and k_- that appear in γ^{ss}_r. Solving Eq. S16 simultaneously we find

$$\langle \delta c_T^2 \rangle = \frac{1}{\Omega} \cdot \frac{1}{\alpha_{ss}} \left[k_c c_{ss} + k_b c b_{ss} + (k_c - k_b)\, \nu_{ss} \cdot \frac{\alpha_{ss} c b_{ss} + k_b c b_\infty}{\alpha_{ss} + k_b} \right] \tag{S19a}$$

$$\langle \delta c_T\, \delta b_T \rangle = \frac{1}{\Omega} \cdot \frac{\alpha_{ss} c b_{ss} + k_b c b_\infty}{\alpha_{ss} + k_b} \tag{S19b}$$

$$\langle \delta b_T^2 \rangle = \frac{b_T^\infty}{\Omega} \tag{S19c}$$

where $\alpha_{ss} = -\beta_{ss}(k_c + k_b w_{ss})$.

Finally, we note that in the $(\delta c, \delta c_T, \delta b_T)$ system, δc is the fast variable and the 3×3 covariance matrix Σ^{fast}_{ss} for the fast subsystem,

$$\Sigma^{fast}_{ss} = \begin{pmatrix} \langle \delta c^2 \rangle & \langle \delta c\, \delta c_T \rangle & \langle \delta c\, \delta b_T \rangle \\ \star & \langle \delta c_T^2 \rangle & \langle \delta c_T\, \delta b_T \rangle \\ \star & \star & \langle \delta b_T^2 \rangle \end{pmatrix}$$

satisfies

$$H^{fast}_{ss} \Sigma^{fast}_{ss} + \Sigma^{fast}_{ss} (H^{fast}_{ss})^T = \Gamma^{fast}_{ss} \tag{S20}$$

where $\langle \delta c_T^2 \rangle$, $\langle \delta c_T\, \delta b_T \rangle$ and $\langle \delta b_T^2 \rangle$ are known. In the rapid buffer limit ($k_+, k_- \to \infty$ with $\kappa = k_-/k_+$ fixed) this matrix equation simplifies considerably, because elements and terms of H^{fast}_{ss} and Γ^{fast}_{ss} that do not involve k_+ and k_- can be dropped, namely,

$$H^{fast}_{ss} = \begin{pmatrix} -\left[k_+ (b_{ss} + c_{ss}) + k_-\right] & k_+ c_{ss} + k_- & -k_+ c_{ss} \\ 0 & 0 & 0 \\ 0 & 0 & 0 \end{pmatrix}$$

and

$$\Gamma^{fast}_{ss} = \begin{pmatrix} \gamma^{ss}_r & 0 & 0 \\ 0 & 0 & 0 \\ 0 & 0 & 0 \end{pmatrix}.$$

Expanding Eq. S20 we write the following three equations for the unknown $\langle \delta c^2 \rangle$, $\langle \delta c\, \delta c_T \rangle$ and $\langle \delta c\, \delta b_T \rangle$,

$$2(h^{fast}_{c\,c} \langle \delta c^2 \rangle + h^{fast}_{c\,c_T} \langle \delta c\, \delta c_T \rangle + h^{fast}_{c\,b_T} \langle \delta c\, \delta b_T \rangle) = -\gamma^{fast}_{c\,c} = -\gamma^{ss}_r \tag{S21a}$$

$$h^{fast}_{c\,c} \langle \delta c\, \delta c_T \rangle + h^{fast}_{c\,c_T} \langle \delta c_T^2 \rangle + h^{fast}_{c\,b_T} \langle \delta c_T\, \delta b_T \rangle = 0 \tag{S21b}$$

$$h^{fast}_{c\,c} \langle \delta c\, \delta b_T \rangle + h^{fast}_{c\,c_T} \langle \delta c_T\, \delta b_T \rangle + h^{fast}_{c\,b_T} \langle \delta b_T^2 \rangle = 0, \tag{S21c}$$

where $\langle \delta c^2 \rangle$, $\langle \delta c\, \delta c_T \rangle$, and $\langle \delta c\, \delta b_T \rangle$ are the unknowns. Combining these three equations, we express $\langle \delta c^2 \rangle$ as a function of the slow covariances,

$$\langle \delta c^2 \rangle = \frac{c_{ss} w_{ss} \beta_{ss}}{\Omega} + \beta_{ss}^2 \left(\langle \delta c_T^2 \rangle - 2\nu_{ss} \langle \delta c_T\, \delta b_T \rangle + \nu_{ss}^2 \langle \delta b_T^2 \rangle \right). \tag{S22}$$

Using Eq. S22, algebraic manipulations allow us to express $\sigma_c' = \langle \delta c^2 \rangle$ in terms of model parameters (Eq. 37). The remaining covariances of the original system with three fast

variables $(\delta c, \delta b, \delta cb)$ can be found through the relationships $\delta c_T = \delta c + \delta cb$, $\delta b_T = \delta b + \delta cb$, and

$$\begin{aligned}
\langle \delta c\, \delta c_T \rangle &= \langle \delta c^2 \rangle + \langle \delta c\, \delta cb \rangle \\
\langle \delta c\, \delta b_T \rangle &= \langle \delta c\, \delta b \rangle + \langle \delta c\, \delta cb \rangle \\
\langle \delta c_T^2 \rangle &= \langle \delta c^2 \rangle + 2\langle \delta c\, \delta cb \rangle + \langle \delta cb^2 \rangle \\
\langle \delta c_T\, \delta b_T \rangle &= \langle \delta c\, \delta b \rangle + \langle \delta c\, \delta cb \rangle + \langle \delta b\, \delta cb \rangle + \langle \delta cb^2 \rangle \\
\langle \delta b_T^2 \rangle &= \langle \delta b^2 \rangle + 2\langle \delta b\, \delta cb \rangle + \langle \delta cb^2 \rangle.
\end{aligned}$$

From the perspective of analytical work, the two-step process of the fluctuating rapid buffer approximation is far easier than solving the Lyapunov equation for the covariance matrix Σ_{ss} for δc, δb and δcb, because the fast and slow versions of the Γ_{ss} and H_{ss} matrices of the RBA are simpler than those of the full calculation.

Appendix C: Analysis of the fluctuating RBA and intrinsic fluctuations

We analyze the Langevin domain model when the exchange rates for Ca^{2+} and buffer are identical ($k_c = k_b = k$). In this case the fluctuating RBA simplifies to

$$\sigma_c' = \frac{c_{ss}}{\Omega} \cdot (1 + \chi) \qquad \chi = \frac{w_{ss}}{(1 + w_{ss})^2} \cdot \frac{c_{ss} - c_\infty}{\kappa + c_\infty}. \tag{S24}$$

Under this restriction, the relative increase in the coefficient of variation due to buffer ($c_v'/c_v^0 = \sqrt{1+\chi}$) remains biphasic through the factor $w_{ss}/(1+w_{ss})^2 = w_{ss}\beta_{ss}^2 = \beta_{ss}(1-\beta_{ss})$ that is a biphasic function of b_T^∞. This result is more easily interpreted when $k_c = k_b = k$ because the equations for the slow variables (Eqs. 34b and 34c) simplify,

$$\begin{aligned}
\dot{\delta c_T} &= -k\, \delta c_T + \xi_{c_T}^{ss}(t) \\
\dot{\delta b_T} &= -k\, \delta b_T + \xi_{b_T}^{ss}(t).
\end{aligned}$$

Though δc_T and δb_T remain correlated because $\xi_{c_T}^{ss}(t)$ and $\xi_{c_T}^{ss}(t)$ are correlated, the Lyapunov equation satisfied by the covariances (Eq. S16) also simplifies and $\langle \delta c_T^2 \rangle$, $\langle \delta c_T\, \delta b_T \rangle$ and $\langle \delta b_T^2 \rangle$ may be calculated independently by solving (cf. Eq. S16),

$$-2k\langle \delta c_T^2 \rangle = -(\gamma_c^{ss} + \gamma_{cb}^{ss}) \qquad -2k\langle \delta c_T\, \delta b_T \rangle = -\gamma_{cb}^{ss} \qquad -2k\langle \delta b_T^2 \rangle = -(\gamma_b^{ss} + \gamma_{cb}^{ss})$$

to find

$$\langle \delta c_T^2 \rangle = \frac{c_{ss} + cb_{ss}}{\Omega} \qquad \langle \delta c_T\, \delta b_T \rangle = \frac{cb_{ss} + cb_\infty}{2\Omega} \qquad \langle \delta b_T^2 \rangle = \frac{b_T^\infty}{\Omega} \tag{S25}$$

where the $c_{ss} + cb_{ss}$ in the numerator of $\langle \delta c_T^2 \rangle$ is the steady state total calcium concentration in the domain, and the dependence of this result on k is hidden in c_{ss} through the steady-state flux balance $j_{in} = k(c_{ss} - c_\infty) + k(cb_{ss} - cb_\infty)$.

The final step in the fluctuating RBA is to calculate the covariances that involve the fast variable δc. These covariances satisfy (see Appendix B),

$$h_{c\,c}^{fast}\langle \delta c^2 \rangle + h_{c\,c_T}^{fast}\langle \delta c\, \delta c_T \rangle + h_{c\,b_T}^{fast}\langle \delta c\, \delta b_T \rangle = -\gamma_r^{ss}/2$$

where $\gamma_r^{ss} = (k_+ c_{ss} \cdot b_{ss} + k_- c b_{ss})/\Omega$ can be written as $\gamma_r^{ss} = 2k_+ c_{ss} \cdot b_{ss}/\Omega$ or $\gamma_r^{ss} = 2k_- c b_{ss}/\Omega$, $h_{cc}^{fast} = -[k_+(b_{ss} + c_{ss}) + k_-]$, $h_{cc_T}^{fast} = k_+ c_{ss} + k_-$ and $h_{cb_T}^{fast} = -k_+ c_{ss}$ (cf. Eq. S21). Dividing through by h_{cc}^{fast} gives

$$\langle \delta c^2 \rangle - \beta_{ss} \langle \delta c \, \delta c_T \rangle + \beta_{ss} \nu_{ss} \langle \delta c \, \delta b_T \rangle = \beta_{ss} w_{ss} c_{ss}/\Omega \tag{S26}$$

where we have used $h_{cc_T}^{fast}/h_{cc}^{fast} = -\beta_{ss}$ and $h_{cb_T}^{fast}/h_{cc}^{fast} = \beta_{ss}\nu_{ss}$ and have written $\nu_{ss} = c_{ss}/(c_{ss} + \kappa) = c b_{ss}/b_T^\infty$ for the steady-state fraction of Ca^{2+}-bound buffer in the domain. The right hand of Eq. S26 that originates from the covariance of ξ_c^{ss} may be expressed in several ways ($w_{ss} c_{ss} = \nu_{ss} b_{ss} = c_{ss} b_{ss}/(c_{ss} + \kappa) = \kappa c b_{ss}/(c_{ss} + \kappa)$). The covariances $\langle \delta c \, \delta c_T \rangle$ and $\langle \delta c \, \delta b_T \rangle$ in Eq. S26 are

$$\begin{aligned}
\langle \delta c \, \delta c_T \rangle &= \beta_{ss} \left(\langle \delta c_T^2 \rangle - \nu_{ss} \langle \delta c_T \, \delta b_T \rangle \right) = \beta_{ss} \left[c_{ss} + c b_{ss} - \nu_{ss} \tfrac{1}{2}(c b_{ss} + c b_\infty) \right] / \Omega \\
\langle \delta c \, \delta b_T \rangle &= \beta_{ss} \left(\langle \delta c_T \, \delta b_T \rangle - \nu_{ss} \langle \delta b_T^2 \rangle \right) = \beta_{ss} \left[\tfrac{1}{2}(c b_{ss} + c b_\infty) - \nu_{ss} b_T^\infty \right] / \Omega.
\end{aligned}$$

Thus, the variance of the fast variable $\langle \delta c^2 \rangle$ can be written in terms of the covariances of the slow variables,

$$\langle \delta c^2 \rangle = \beta_{ss} \left[w_{ss} \frac{c_{ss}}{\Omega} + \beta_{ss} \left(\langle \delta c_T^2 \rangle - 2\nu_{ss} \langle \delta c_T \, \delta b_T \rangle + \nu_{ss}^2 \langle \delta b_T^2 \rangle \right) \right] \tag{S27}$$

and it can be shown that $\langle \delta c \, \delta b_T \rangle$ is negative while $\langle \delta c \, \delta c_T \rangle$ and $\langle \delta c^2 \rangle$ are positive. Upon substitution of Eq. S25, we have

$$\begin{aligned}
\langle \delta c^2 \rangle &= \frac{\beta_{ss}}{\Omega} \left\{ w_{ss} c_{ss} + \beta_{ss} \left[c_{ss} + c b_{ss} - \nu_{ss}(c b_{ss} + c b_\infty) + \nu_{ss}^2 b_T^\infty \right] \right\} && \text{(S28a)} \\
&= \frac{1}{\Omega} \left\{ (1 - \beta_{ss}) c_{ss} + \beta_{ss}^2 \left[c_{ss} + c b_{ss} - \nu_{ss}(c b_{ss} + c b_\infty) + \nu_{ss}^2 b_T^\infty \right] \right\}. && \text{(S28b)}
\end{aligned}$$

This analysis of the fluctuating RBA under the restriction $k_c = k_b$ shows that an increase in total buffer b_T^∞ increases the absolute value of the slow covariances (Eq. S25). These covariances (the terms within square brackets in Eq. S28) combine to create a net positive impact on $\langle \delta c^2 \rangle$ that is attenuated to some extent by a decrease in the β_{ss} that scales these terms. The β_{ss}/Ω outside the curly brackets in Eq. S28a might be interpreted as an effective volume that attenuates all of these contributions to $\langle \delta c^2 \rangle$, but this is misleading because $\beta_{ss} w_{ss} c_{ss} = (1 - \beta_{ss}) c_{ss}$ is an increasing function of b_T^∞ (cf. Eq. S28b). Furthermore, Eq. S24 shows that the variance of the free $[Ca^{2+}]$ fluctuations in the presence of buffer $b_T^\infty > 0$ is never less than what would occur in the absence of buffer ($b_T^\infty = 0$).

SUPPORTING REFERENCES

1. Gillespie, D., 2007. Stochastic simulation of chemical kinetics. *Annual review of physical chemistry* 58:35-55.

2. Laub, A. J., 2004. Kronecker Products. *In* Matrix Analysis for Scientists and Engineers, Society for Industrial and Applied Mathematics.

3. Keizer, J., 1987. Statistical Thermodynamics of Nonequilibrium Processes. Springer Verlag.

4. Gillespie, D. T., 2000 The chemical Langevin equation. *Journal of Chemical Physics* 113:297-306.

5. Higham, D. J., 2008 Modeling and simulating chemical reactions. *SIAM Review* 50:347-368.

6. Gardiner, C.W., 1997 Handbook of Stochastic Methods for Physics, Chemistry, and the Natural Sciences. Springer Verlag, New York.

7. Van Kampen, N. G., 1981. Stochastic Processes in Physics and Chemistry. North-Holland Publishing Company, Amsterdam.